

# EXPERIMENTAL AND NUMERICAL INVESTIGATION OF 2D PALISADE FLUTTER FOR THE HARMONIC OSCILLATIONS

Vladymir Tsimbalyuk, Anatoly Zinkovskii

*Institute for Problems of Strength, Ukrainian National Academy of Sciences  
Ukrainian National Academy of Sciences, 2 Timiriazevskaia str., 01014 Kiev, Ukraine  
tsymb@yahoo.com*

Vitaly Gnesin

*Department of Aerohydromechanics, Institute for Problems in Machinery  
Ukrainian National Academy of Sciences, 2/10 Pozharsky st., Kharkov 310046, Ukraine  
gnesin@ipmach.kharkov.ua*

Romuald Rzadkowski, Jacek Sokolowski

*Institute of Fluid-Flow Machinery, Polish Academy of Sciences  
80-952 Gdansk, ul. Fiszera 14, Polish Naval Academy  
z3@imp.gda.pl*

**Abstract** The verification of the computational models for unsteady flows through the oscillating blade row becomes more difficult, because the experimental data for three-dimensional flows are currently hardly available in the published literature. Therefore comparisons between numerical methods and experimental ones for simple cascade geometry at inviscid flow conditions must play an essential role in validation of the three-dimensional unsteady solution methods. In this study the numerical calculations were performed to compare the theoretical results with experiments for the harmonic motion. The calculations were carried out for the torsional and bending oscillations of the compressor cascade. The comparison of the calculated and experimental results for different conditions of the cascade oscillations has shown the good quantitative and qualitative agreement.

**Keywords:** flutter, inviscid, blades

## 1. Introduction

Cases of flutter-type instability are sometime encountered in the course of developing new gas turbine engines. Costly testing is necessary to eliminate this problem. One of the main problems in predicting flutter at the engine design stage is determining the transient aerodynamic loads that develop during the vibrations of blades. This problem is particularly important in the case of separated flow, when theoretical methods of determining the transient aerodynamic loads are not yet sufficiently reliable. Thus, in this study, we use an experimental method of determine the transient aerodynamic loads on the vibrating blades of turbine engine.

It is quite difficult to measure the aerodynamic loads along the blades during rotation of the blading ring. Thus, with allowance for the three-dimensional nature of the air flow about the ring, the cylindrical sections of the ring are often modeled as vane cascades. When such a cascade is placed in a wind tunnel, the flow parameters, geometric characteristics, and vibration parameters should be constant along the vanes.

The aeroelastic results of bending vibrations of 2D linear cascade in subsonic flow were published by Kaminier and Stel'makh 1996 and torsional Kaminier et al. 1988. The experimental results of aero-damping and dynamic stability of compressor cascades under bending-torsional vibrations were presented in Len et al. 1986.

Useful benchmark data, which became a de facto standard for unsteady cascade flows, can be found in Bölcs and Fransson 1986 for the EPFL series of Standard configurations.

Aerodynamic loads are measured indirectly either through the aerodynamic damping of bladed vibrations by Kaminier and Nastenka 1973 or the distribution of transient pressures on the blade surfaces Tanaka et al. 1984. They are measured directly with an extensometric dynamometer Kimura and Nomiyama 1988 or on the basis of the forces developed by vibrators Kaminier et al. 1988.

In the Institute for Problem of Strength of NAS of Ukraine the proper 2D experimental bench was developed to measure simultaneously unsteady aerodynamic force and moment with arbitrary combinations of motions  $y$  and  $a$  of airfoil cascades in the subsonic flow. Description of such test bench is given in paper Tsimbalyuk et al. 2002.

## 2. Test Stand

To realize flow about the vane cascade with prescribed velocities and angles of attack, the cascade was placed in a wind tunnel (Figures 1, 2) in which Mach numbers up to 0.7 could be attained. The four central vanes in the cascade were secured to individual vibration units and could undergo prescribed vibrations with two degrees of freedom. Since there was some mechanical

coupling even with vibration-proofing elements between the units, it was necessary to keep the vibrations in all of the units steady (whether there was a flow or not) in order to prevent this coupling from affecting the measurement results. Proceeding on the basis of this requirement, we employed an eight-channel feedback system to automatically control the vibrations of the vanes (vibration units). The system also controls the voltages and, thus, the forces on the vibrator coils so as to reduce the difference between the signal of the master oscillator and the vane vibration signal obtained in each channel (the equipment used was described in more detail in Tsymaluk 1996).

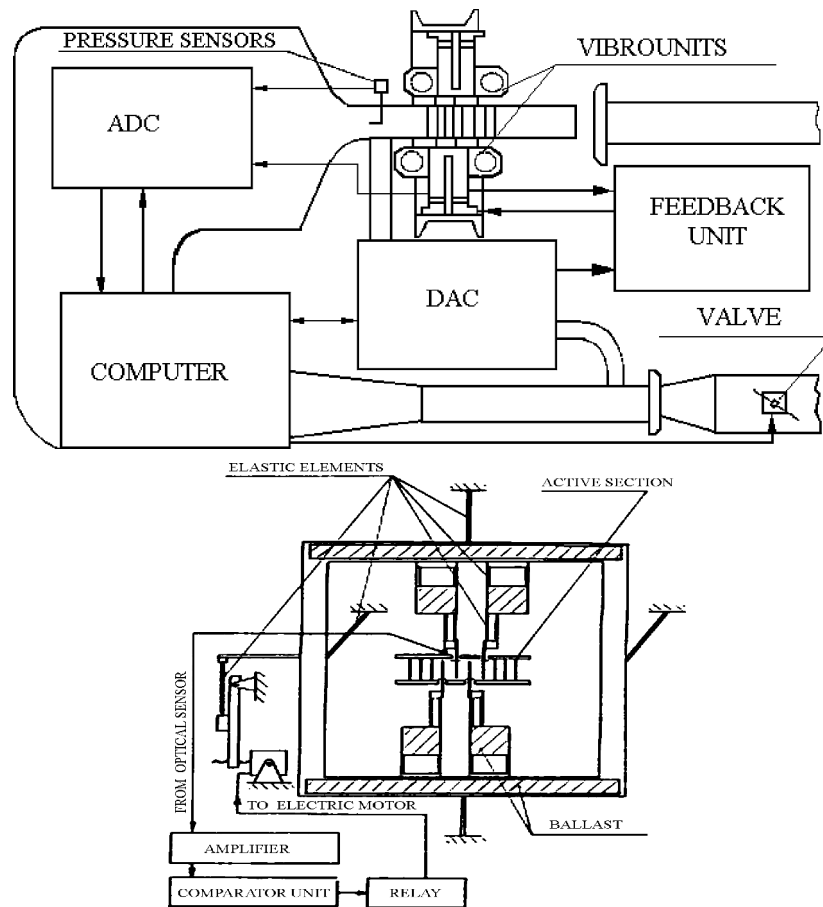


Figure 1. Test stand

The considered cascade consists of 9 airfoils. The central three were fastened cantilever on the individual vibro-unit (see Figure 3), they could accomplish assigned displacements, aerodynamic loads were measured on them. Such airfoils are called active. An elastic suspension was designed for vanes that has two elastic elements of different widths. The auxiliary (narrow) elas-

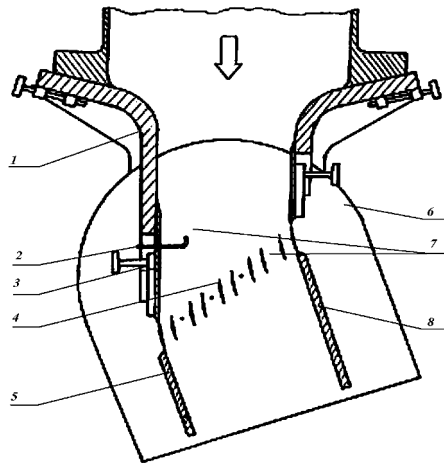


Figure 2. Linear Test Facility, 1 - nozzle wall; 2 - Pito tube; 3 - blade; 4 - airfoil; 5,8 - outlet rotary screens; 6 - rotary disk; 7 - openings for static pressure release

tic element does not impede the twisting of the main (wide) element about its own longitudinal axis, and during flexural vibrations the two elements form an elastic parallelogram. This setup ensures constant vibration parameters along the vane. The unit just described also makes it possible to change the natural frequencies of the suspension by using replaceable main elements differing only in thickness.

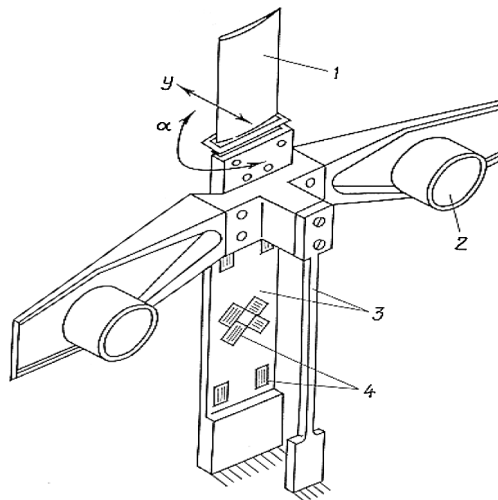


Figure 3. Structure of the airfoil flexible suspension 1 - airfoil; 2 - voice coil of the vibrator; 3 - elastic elements; 4 - strain gages

There were used three active airfoils to asset aerodynamic loads on initial airfoil ( $n=0$ ), which were induced by vibration of airfoils -2, using designed experimental workbench. This could be accounted for periodicity of influence of airfoil  $n = -1$  on  $n = 1$  one to be the same as for  $n = -2$  on  $n = 0$ , influence of  $n = 1$  airfoil on  $n = -1$  - the same as for  $n = 2$  on  $n = 0$  airfoil.

In accordance with developed method, the required vibrations were induced for every active airfoil. The first harmonic of the unsteady aerodynamic force and moment was measured on them. It should be noted, that determined unsteady aerodynamic forces and moments, and thus aerodynamic influence coefficients (AIC) were related to the center of airfoil chord, about which its angular displacement occurred.

The geometrical characteristics of the compressor cascade and oscillation regimes are presented by Tsimbalyuk et al. 2002. The blade length  $L=0.069$  m, the chord length  $b= 0.05$  m, the circular camber  $10^\circ$ , the thickness-to chord ratio 0.07, the stager angle 60 deg., pitch-to -chord ration 0.78, the inlet Mach number 0.12 -0.35, the vibration amplitude  $h_o =0.0007$  m,  $\alpha_o =0.0084$  rad. The cross-section of the blade is presented in Figure 4.

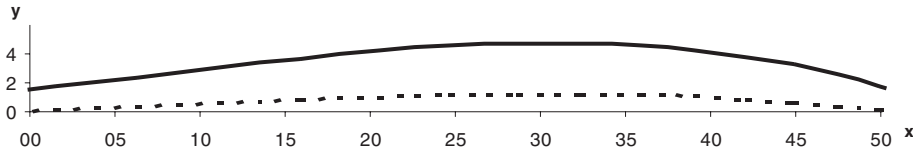


Figure 4. Airfoil coordinates, solid line-suction side, dashed line -pressure side

In order to calculate the AIC the vibrations of airfoils were induced by turns. The vibration amplitude of the blade was almost invariable along its length and equal to  $\omega = 85.85$  Hz, which is equal to the natural frequency of the system.

### 3. Aeroelastic Model

Let assume that the blades are non-twisted with a constant cross-sectional area along the blade length. The centre of shear and gravity of the blade cross-sections coincide. Let us consider the motion of  $n$ th blade as plane motion of the solid body with two degrees of freedom. The transverse displacements of the  $n$ th blade in  $x, y$  directions ( $h_{x_n}, h_{y_n}$ ) are described as:

$$h_{x_n}(t) = h_{x_0} \sin[\omega_n t + (n - 1)\delta],$$

$$h_{y_n}(t) = h_{y_0} \sin[\omega_n t + (n-1)\delta],$$

and angular displacements of the  $n$ th blade  $\alpha_n(t)$ :

$$\alpha_n(t) = \alpha_0 \sin[\omega_n t + (n-1)\delta]. \quad (1)$$

Here  $h_{x_0}, h_{y_0}, \alpha_0$  are the amplitudes of oscillations the same for all blades;  $\omega_n$  is oscillation angular frequency of the  $n$ th blade;  $\delta$  is the constant interblade phase angle;  $n$  is the blade number.

The equations of motion are reduced to set of three ordinary linear differential equations of first order for only torsion ( $\alpha_n$ ) and bending ( $h_{x_n}, h_{y_n}$ ). For a constant force  $\mathbf{F}_o$  acting during a period  $\Delta t$  one obtains the linear differential equations of second order with the constant coefficients for  $n$ -th blade:

$$\ddot{h}_{x_n} + 2n_n \dot{h}_{x_n} + \omega_n^2 h_{x_n} = \frac{f_{xn}}{m_n}, \quad (2)$$

$$\ddot{h}_{y_n} + 2n_n \dot{h}_{y_n} + \omega_n^2 h_{y_n} = \frac{f_{yn}}{m_n}, \quad (3)$$

$$\ddot{\alpha}_n + 2n_n \dot{\alpha}_n + \omega_n^2 \alpha_n = \frac{M_{sn}}{m_n}, \quad (4)$$

where  $n_n$  is a damping parameters.

The 3D unsteady transonic flow of an ideal gas is described by the Euler equations, represented as conservation laws in an arbitrary Cartesian coordinate system, rotating with the constant angular velocity  $\omega$  (see Gnesin and Rzadkowski 2000):

$$\frac{\partial}{\partial t} \int_{\Omega} \mathbf{f} d\Omega + \oint_{\sigma} \mathbf{F} \cdot \mathbf{n} d\sigma + \int_{\Omega} \mathbf{H} d\Omega = 0,$$

$$\mathbf{f} = \begin{bmatrix} \rho \\ \rho v_1 \\ \rho v_2 \\ \rho v_3 \\ E \end{bmatrix}; \mathbf{F} = \begin{bmatrix} \rho \mathbf{v} \\ \rho v_1 \mathbf{v} + \delta_{1i} p \\ \rho v_2 \mathbf{v} + \delta_{2i} p \\ \rho v_3 \mathbf{v} + \delta_{3i} p \\ (E + p) \mathbf{v} \end{bmatrix}; \mathbf{H} = \begin{bmatrix} 0 \\ \rho a_{e1} - 2\rho\omega v_2 \\ \rho a_{e2} - 2\rho\omega v_1 \\ 0 \\ 0 \end{bmatrix}; \delta_{ji} = \begin{cases} 1 & j = i \\ 0 & j \neq i \end{cases} \quad (3)$$

Here  $p$  and  $\rho$  are the pressure and density;  $v_1, v_2, v_3$  are the velocity components;  $a_{e1}$  and  $a_{e2}$  are the transfer acceleration projections;  $E = \rho \left( \varepsilon + \frac{v_1^2 + v_2^2 + v_3^2 + r^2 \omega^2}{2} \right)$  is the total energy of volume unit;  $\varepsilon$  is an internal energy of mass unit;  $r$  is the distance from the rotation axis.

The above system of equations is completed by the perfect gas state equation

$$p = \varepsilon(\chi - 1),$$

where  $\chi$  denotes the ratio of the fluid specific heats.

The spatial solution domain is discretized using linear hexahedral elements.

The 3D Euler equations are integrated on moving H-H (or H-O) - type grid with use of explicit monotonous second - order accuracy Godunov - Kolgan difference scheme.

#### 4. Numerical and Experimental Results

The aeroelastic behavior of the system "fbw-cascade" without taking into account the mechanical damping is defined by a the work coefficient value which is equal to the work performed by aerodynamic forces during one cycle of oscillations:

$$W = \int_0^{\frac{1}{\nu}} M \frac{d\alpha}{dt} dt, \quad (5)$$

where  $c$  is the length of blade chord,  $\alpha_0$  is oscillation amplitude,  $M$  is aerodynamical moment,  $W$  is the aerodynamic work during one cycle of oscillation for torsional oscillations, and

$$W = \int_0^{\frac{1}{\nu}} -\mathbf{F} \cdot \mathbf{v} dt, \quad (6)$$

for bending oscillations.

The work coefficients versus interblade phase angle (IBPA) for different fbw regimes and modes of oscillations are presented in Figures 5-7.

Figure 5 shows the work coefficient as function of IBPA for bending oscillations under incidence fbw angle which is equal to zero. The light squares (circles) correspond to the experimental data, the black squares (circles) correspond to numerical results. The negative values of work coefficient demonstrate the dissipation of an oscillating blade energy to the fbw (aerodamping), the positive values - to the transfer of the energy from the main fbw to the blade (flutter).

The strong influence of both IBPA and Strouhal number on the aerodynamic stability of tune modes is seen in Figure 5. With decreasing of Strouhal number (increasing of the inlet fbw velocity) the stability decreases.

It should be noted that the work coefficient in dependence of IBPA has a typical sinusoidal form. At the IBPA equal to 180 deg the maximal aerodamping is observed, at the IBPA near 0 deg the minimal aerodamping is found.

The quantitative and qualitative agreement between predicted and measured values is satisfactory.

In Figure 6 the variation of work coefficient versus IBPA for torsional oscillations under  $i = 0$  and  $Sh = 0.616$  is shown. The agreement between theoretical

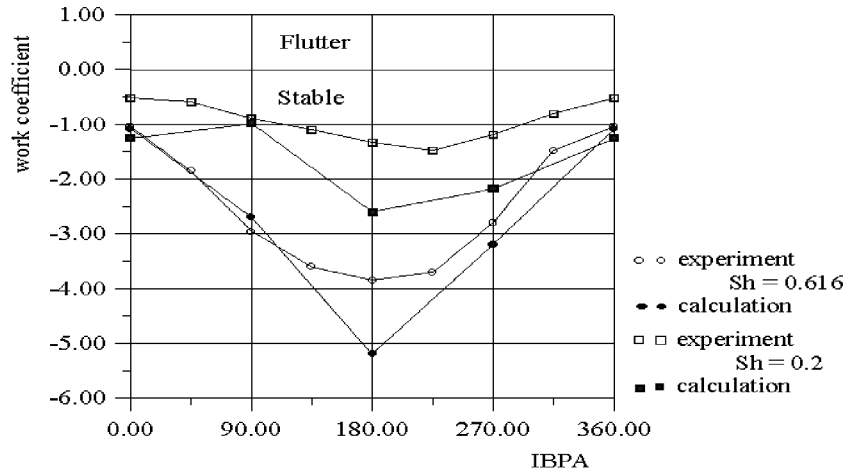


Figure 5. The aerodynamic work coefficient in dependence of IBPA for the bending vibration ( $i = 0^\circ$ , Strouhal Number -  $Sh = 0.2 - 0.616$ )

and experimental results is good. For torsional oscillations in the range of  $0 \text{ deg.} < \text{IBPA} < 180 \text{ deg.}$  the work coefficients have positive value that corresponds to the transfer of energy from the flow to the oscillating blade. The maximal excitation occurs near  $\delta = +90 \text{ deg.}$

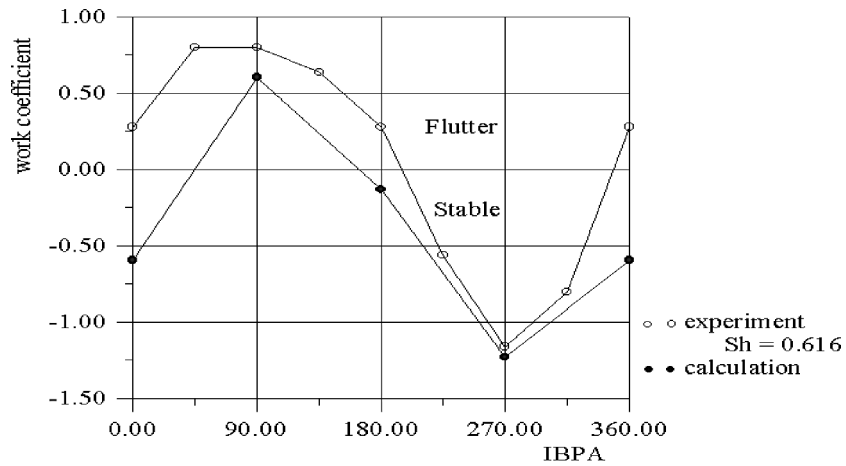


Figure 6. The aerodynamic work coefficient in dependence of IBPA for torsion vibration ( $I = 0^\circ$ , Strouhal Number -  $Sh = 0.616$ )

The aeroelastic characteristics at the bending vibration for the attack flow angle of  $16 \text{ deg}$  is presented in Figure 7. The agreement between the exper-



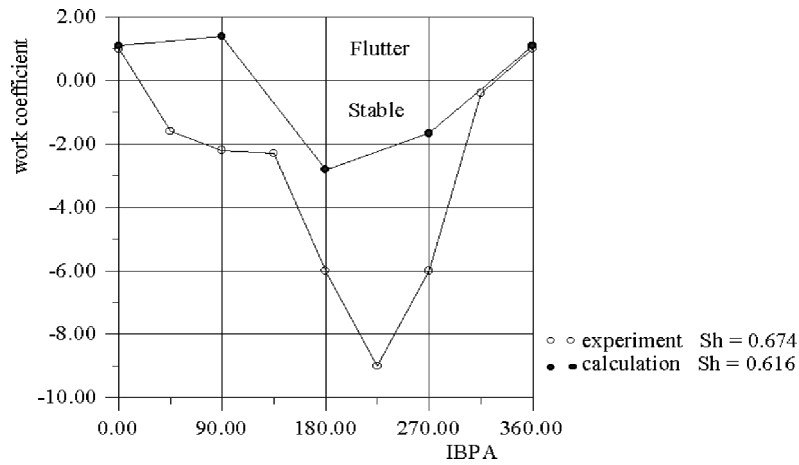


Figure 7. Aerodynamic work coefficient in dependence of IBPA for the bending vibration ( $i = 16^\circ$ , Strouhal Number -  $Sh = 0.616$ )

imental and numerical results near the IBPA of 0 deg is seen although some discrepancy for IBPA of 180 deg is found.

In Figures 8, 9 and 10 the calculated and measured amplitude of unsteady forces at the bending oscillations, for different incidence angles were shown. The calculation of the unsteady amplitude by using the aerodynamic influence coefficients were done taking into account only four neighbouring blades ( $-1 \leq n \leq 1$ ) and two neighbouring blades ( $-2 \leq n \leq 2$ ). From results presented in these Figures it is seen that for considered fbw regime taking into account only two neighbouring blades give the satisfactory agreement with numerical calculations.

## 5. Conclusions

1. A partially - integrated method based on the solution of the coupled aerodynamic-structure problem is used for calculation of unsteady 3D fbw through an oscillating blade row to determine the critical conditions of flutter initiation.
2. The numerical investigation has been performed to calculate aeroelastic response of the compressor cascade at the different fbw regimes and laws of oscillations.
3. The comparison of calculated and experimental results for bending and torsional oscillations has shown a satisfactory quantitative and qualitative agreement.

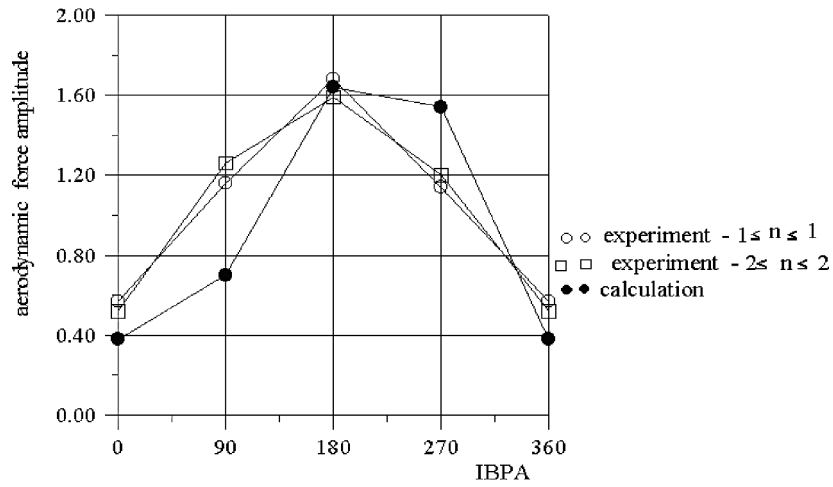


Figure 8. Amplitude of unsteady aerodynamic force at the bending oscillations

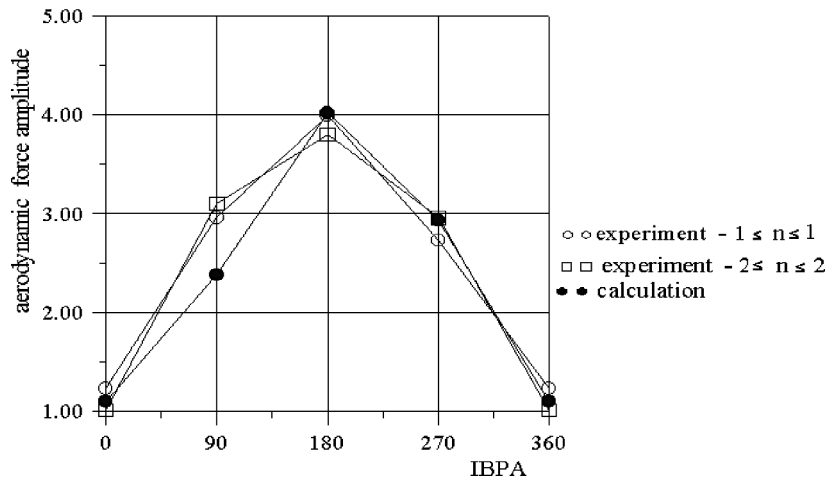


Figure 9. Amplitude of unsteady aerodynamic force at the bending oscillations  $i = 0$ ,  $Sh = 0.616$

## References

- Bölcs A., Fransson T.H. (1986) Aeroelasticity in Turbomachines Comparison of Theoretical and Experimental Cascade Results, Communication du Laboratoire de Thermique Appliquée et Turbomachines, Nr.13. Lusanne, Epfel.
- Bölcs A., and Fransson T.H. (1986). Aeroelasticity in Turbomachines Comparison of Theoretical and Experimental Cascade Results, Communication du Laboratoire de Thermique Appliquée et Turbomachines, Nr.13, Appendix A5 All Experimental and Theoretical Results for the 9 Standard Configurations, Lusanne, Epfel.

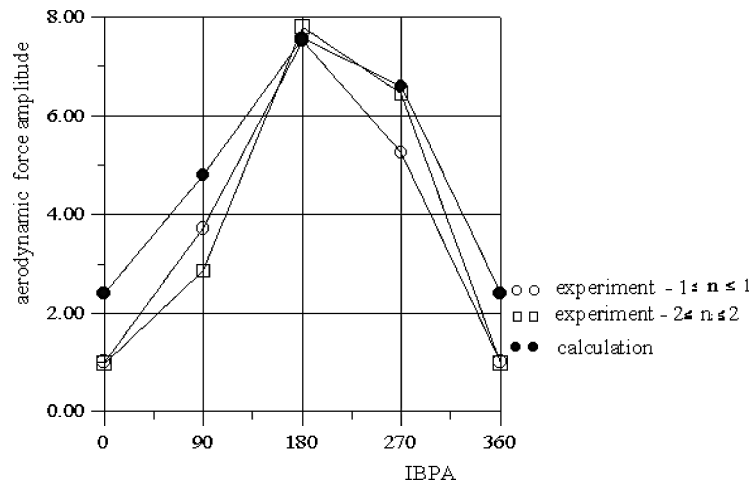


Figure 10. Amplitude of unsteady aerodynamic force at the bending oscillations  $i = 16$ ,  $Sh = 0.616$

- Stel'makh A.L., Kaminer A.A. (1981). Effect of the geometrical parameters of a compressor cascade on the limit of bending self-oscillations of blades caused by cascade flutter, *Strength of Materials*, 15, 1, 104-109.
- Kaminer A.A., Stel'makh A.L. (1996). Effect of the aerodynamic connectedly between blades of the aerodynamic damping of their vibrations, and origin of cascade flutter, *Strength of Materials*, 14, 12, 1667-1672.
- Kaminer A.A., Chervonenko A.G., and Tsymbalyuk V.A. (1988). Method for Studying Unsteady Aerodynamic Characteristics of Airfoil Cascades vibrating in a Three-Dimensional Flow. Preprint. Institute for Problems of Strength, Ac. Sci. of the Ukr.SSR, Kiev 1988 (in Russian).
- Len A.D., Kaminer A.A., Stel'makh A.L., Balalaev V.A. (1986). Loss of dynamic stability of torsional vibrations of blades due to cascade flutter, *Strength of Materials*, 18, 1, 76-80.
- Gnesin V., and Rzakowski R. (2000). The theoretical model of 3D flutter in subsonic, transonic and supersonic inviscid flow, *Transactions of the Institute of Fluid-Flow Machinery*, No. 106, 45-68.
- Gnesin V., Rzakowski R. (2002). A Coupled Fluid-Structure Analysis for 3D Inviscid Flutter of IV Standard Configuration, *Journal of Sound and Vibration*, 251(2), 315-327.
- Gnesin V., Rzakowski R. and Kolodyazhnaya, L., V. (2000). A coupled fluid-structure analysis for 3D flutter in turbomachines, ASME paper 2000-GT-0380.
- Rzakowski R., Gnesin V. (2000). The numerical and experimental verification of the 3D inviscid code, *Transactions of the Institute of Fluid-Flow Machinery*, No. 106, 2000, 69-95.
- Rzakowski R. (1998). Dynamics of steam turbine blading. Part two: Bladed discs, Ossolineum, Wrocław-Warszawa.
- Tsymbalyuk V.A. (1996). Method of measuring transient aerodynamic forces and moments on vibrating cascade, *Strength of Materials*, 28, 2, 150-157.
- Tsymbalyuk V.A., Zinkovski A.P and Rzakowski R. (2002). Experimental Investigation of Palisade Flutter for the Harmonic Oscillations, *Proc. of the XV Conference of Flow Mechanics*, Augustow, Poland